

Faster-than-Bohm Cross- \mathbf{B} Electron Transport in Strongly Pulsed Plasmas

N. Brenning,¹ R. L. Merlino,² D. Lundin,³ M. A. Raadu,¹ and U. Helmersson³

¹*Division of Space and Plasma Physics, EE, Royal Institute of Technology, SE-100 44 Stockholm, Sweden*

²*Department of Physics and Astronomy, University of Iowa, Iowa City, Iowa 52242, USA*

³*Plasma and Coatings Division, IFM-Materials Physics, Linköping University, SE-581 83 Linköping, Sweden*

(Received 20 August 2009; published 25 November 2009)

We report the empirical discovery of an exceptionally high cross- \mathbf{B} electron transport rate in magnetized plasmas, in which transverse currents are driven with abruptly applied high power. Experiments in three different magnetic geometries are analyzed, covering several orders of magnitude in plasma density, magnetic field strength, and ion mass. It is demonstrated that a suitable normalization parameter is the dimensionless product of the electron (angular) gyrofrequency and the effective electron-ion momentum transfer time, $\omega_{ge}\tau_{\text{EFF}}$, by which all of diffusion, cross-resistivity, cross- \mathbf{B} current conduction, and magnetic field diffusion can be expressed. The experiments show a remarkable consistency and yield close to a factor of 5 greater than the Bohm-equivalent values of diffusion coefficient D_{\perp} , magnetic-diffusion coefficient D_B , Pedersen conductivity σ_P , and transverse resistivity η_{\perp} .

DOI: 10.1103/PhysRevLett.103.225003

PACS numbers: 52.72.+v, 52.35.-g, 52.50.Dg, 52.55.Ez

Electron cross- \mathbf{B} transport in plasmas is often much faster than classically predicted through collisions. One example is Bohm diffusion [1] which, besides a fast diffusion rate, has the property to scale inversely with the magnetic field strength, in contrast to classical diffusion that scales inversely as the square of the magnetic field strength. Although empirically discovered in the 1940s, Bohm diffusion is still a topic of interest today. Diffusion at, or even faster than, the Bohm rate has recently been reported from as widely different situations as the scrape-off layer of the RFX fusion experiment [2], basic-plasma experiments on particle transport [3], observations of reconnection in Earth's magnetotail by the Cluster spacecraft [4], theoretical estimates of the maximum possible rate of relativistic reconnection [5], and the acceleration of high energy (10^{15} eV and beyond) galactic cosmic rays in the shock waves of young supernova remnants [6]. In the latter context, data from five young supernova remnants even show that “values typically between 1 and 10 times the Bohm diffusion coefficient are found to be required” [7]. It is thus clear that there is a need to understand diffusion beyond the Bohm value.

We report here on an extended evaluation of the cross- \mathbf{B} electron transport properties in four experiments in magnetized plasmas that are strongly pulsed in various ways, and put the various types of data in a common theoretical frame. The experiments are of three different kinds: a plasma penetration experiment, two pulsed sputtering magnetrons, and a toroidal theta pinch. In three of them we have access to the original data and a detailed knowledge of the devices. The focus of this extended evaluation is on the anomalous magnetic and electron diffusion coefficients D_B and D_{\perp} and the Pedersen and Hall cross- \mathbf{B} conductivities σ_P and σ_H . From each of these we extract three transport parameters that reflect the common underlying physics of plasma cross-resistivity [1,8]. These pa-

rameters are the cross-resistivity itself η_{\perp} , the effective electron momentum transfer time τ_{EFF} , and its product $\omega_{ge}\tau_{\text{EFF}}$ with the electron (angular) gyrofrequency $\omega_{ge} = eB/m_e$. Provided that n_e and B are known, all of D_B , D_{\perp} , σ_H , and σ_P can be expressed as functions of η_{\perp} , τ_{EFF} , or $\omega_{ge}\tau_{\text{EFF}}$.

Experimentally obtained values of τ_{EFF} from four different experiments are plotted against the magnetic field strength in Fig. 1. It reveals an inverse proportionality such that $\tau_{\text{EFF}} \propto 1/B$. The dashed lines show $\tau_{\text{EFF}}(B)$ for constant values of $\omega_{ge}\tau_{\text{EFF}}$ which has the same scaling.

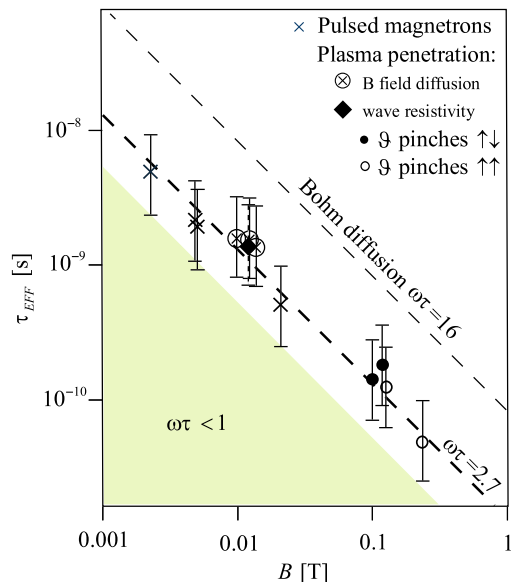


FIG. 1 (color online). The effective momentum transfer time τ_{EFF} as function of the magnetic field strength, obtained from three different types of pulsed plasma experiments. For reference, a dashed line at $\omega_{ge}\tau_{\text{EFF}} \approx 16$, corresponding to Bohm diffusion, is also drawn.

Over 2 orders of magnitude in magnetic field strength, all experiments correspond to $\omega_{ge}\tau_{\text{EFF}}$ within a factor of 1.6 from the common average $\langle\omega_{ge}\tau_{\text{EFF}}\rangle \approx 2.7$. This is remarkable in view of the fact that the experiments together cover large variations of various kinds: (1) length scales of the magnetic field gradients from $l_B < r_{gi}$ in the sputtering magnetrons, $l_B \sim r_{gi}$ in the theta pinches, to $l_B > r_{gi}$ in the plasma penetration experiment, (2) a magnetic null line in the theta pinch $\uparrow\downarrow$ bias case but not in the other experiments, (3) a degree of magnetic perturbation through internal currents from $<1\%$ in the 1.5 kW magnetron to $>200\%$ in the theta pinch experiments, (4) plasma densities from $\sim 10^{17} \text{ m}^{-3}$ in the 1.5 kW magnetron to $>10^{20} \text{ m}^{-3}$ in the theta pinch experiments, (5) ion masses from 1 amu in the plasma penetration experiment to 83 amu in the 70 kW magnetron, and (6) different types of driving energy sources: electric for the magnetrons, magnetic for the theta pinches, and kinetic for the plasma penetration experiment.

The methods of derivation of τ_{EFF} in Fig. 1 differ from case to case, but are all based on Eqs. (1)–(3) below that relate τ_{EFF} to parameters that are determined by measurements, such as the cross- \mathbf{B} current densities, the plasma density, the magnetic field strength, and the magnetic field diffusion coefficient. In the plasma penetration experiment [9], a plasma stream with a speed $v_0 \approx 3 \times 10^5 \text{ m/s}$ was created in a conical theta pinch and shot at a region in which the magnetic field had a transverse component $B_y = -15 \text{ mT}$. It is earlier known [9] that the transverse component of the magnetic field penetrates into the plasma about 2 orders of magnitude faster than the classical magnetic field diffusion time $\tau_B = \mu_0 L^2 / (4\eta_{\text{Sp}}) \approx 100 \mu\text{s}$, where L is the width of the stream and η_{Sp} is the classical Spitzer transverse resistivity. We have used here earlier published [9] profiles of magnetic penetration into plasma streams of three different densities to calculate the magnetic-diffusion coefficients D_B , and from these, using Eq. (3), obtained the three magnetic-diffusion values of τ_{EFF} . The wave-resistivity value in Fig. 1 is obtained by a calculation of η_{\perp} from measured wave data as described in [9]. In the pulsed sputtering magnetron experiments we have used data from two different devices [10,11], with applied peak powers of 1.5, 70, and 300 kW. In these devices, currents flow across the magnetic field in an azimuthal closed current loop \mathbf{J}_{φ} that is perpendicular to the externally closed discharge current \mathbf{J}_D . Measurements of the current density ratio J_{φ}/J_D can be used [8,10] to obtain the ratio between the Hall and the Pedersen conductivities, σ_H/σ_P . We have used four such measurements and from them, taking σ_H and σ_P from Eq. (1), extracted the magnetron values of τ_{EFF} in Fig. 1. Finally, we have used data from the toroidal theta pinch “Thor” at the University of Maryland [12]. A fast rising magnetic pulse ($\partial B/\partial t \sim 10^6 \text{ T/s}$) was here applied to a plasma already having an embedded axial bias magnetic field ($\leq 0.1 \text{ T}$). During the implosion, a magnetic piston in the form of a

current sheath propagates toward the magnetic axis. Depending on the relative polarity of the bias and main magnetic fields the configuration can be either parallel ($\uparrow\uparrow$) or antiparallel ($\uparrow\downarrow$). Here, we have evaluated the magnetic field diffusion constant D_B from the speeds and the profiles of the current sheaths. This yields four values of D_B , two for $\uparrow\uparrow$ bias and two for $\uparrow\downarrow$. From these, Eq. (3) gives four values of τ_{EFF} .

Figure 2 shows that the mechanism, or mechanisms, at work here gives close to the maximum electron cross- \mathbf{B} drift speeds that can be obtained by varying $\omega_{ge}\tau_{\text{EFF}}$. Consider the drift speeds $\mathbf{u}_{e\perp}$, in the direction of the transverse components of the electric, and pressure gradient, volume forces on the electrons: $-en_e\mathbf{E}$ and $-\nabla p_e$. These drift speeds are proportional to σ_P and D_{\perp} , respectively, and can be expressed [1,8] as functions of $\omega_{ge}\tau_{\text{EFF}}$. Figure 2 shows $\sigma_P(\omega_{ge}\tau_{\text{EFF}})$ and $D_{\perp}(\omega_{ge}\tau_{\text{EFF}})$ normalized to their maximum values. The experimental average $\langle\omega_{ge}\tau_{\text{EFF}}\rangle \approx 2.7$ from Fig. 1 corresponds to $\sim 70\%$ of these maximum values. It is interesting to note that the experimental data are gathered close to, but do not enter, the parameter range $\omega_{ge}\tau_{\text{EFF}} < 1$ (highlighted in Figs. 1 and 2 by shaded areas) where both σ_P and D_{\perp} begin to decrease with decreasing τ_{EFF} . In summary, we have strong empirical evidence that there exists a resistive mechanism, or a class of mechanisms, that can be driven by pulsed power in a wide range of situations and parameters, and that reduces the effective momentum transfer time τ_{EFF} just enough to reach close to the theoretical maximum electron cross- \mathbf{B} transport speed, but does not go below that value. The resistive mechanism is so far quantitatively understood only in the plasma penetration experiment where there is a strong correlation between electric field oscillations and plasma density oscillations. As shown in [9] the force on the electrons from the wave structure gives an effective anomalous transverse resistivity η_{EFF} , and a value of τ_{EFF} . The good agreement with the magnetic-diffusion values of τ_{EFF} in Fig. 1 confirms that these oscillations provide the resistive mechanism in the magnetic-diffusion process.

Method.—The electron motion obeys the generalized Ohm’s law [1], of which we here consider only the com-

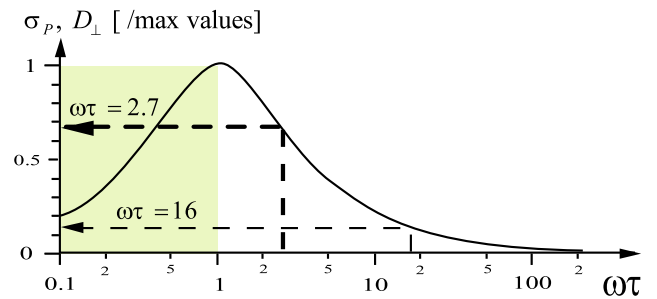


FIG. 2 (color online). The normalized Pedersen conductivity σ_P and the cross- B electron diffusion coefficient D_{\perp} , as functions of $\omega_{ge}\tau_{\text{EFF}}$.

ponents across \mathbf{B} . For phenomena much slower than the electron gyrotome it can be written as $en_e\eta_{\text{EFF}}\mathbf{J} + \mathbf{J} \times \mathbf{B} = en_e(\mathbf{E} + \mathbf{v} \times \mathbf{B}) + \nabla p_e$. This is essentially an equation of motion for the electrons, with the “externally applied” volume force $\mathbf{F}_{\text{TOT}} = en_e(\mathbf{E} + \mathbf{v} \times \mathbf{B}) + \nabla p_e$ on the right-hand side. The $\eta_{\text{EFF}}\mathbf{J}$ term represents the internal resistive force on the electrons along the direction of the current. It corresponds to an effective collision time, or more precisely effective momentum transfer time, $\tau_{\text{EFF}} = m_e/(\eta_{\text{EFF}}e^2n_e)$. If only the ∇p_e force term is retained to the right, it becomes an equation for the diamagnetic current density and the diffusion speed, and with only the $en_e\mathbf{E}$ term an equation for electric conduction. Using these relations, and the electron (angular) gyrofrequency $\omega_{\text{ge}} = eB/m_e$, it is straightforward to derive the electron transport coefficients in a form suitable for the analysis here:

$$\sigma_P = \frac{en_e}{B} \frac{\omega_{\text{ge}}\tau_{\text{EFF}}}{1 + \omega_{\text{ge}}^2\tau_{\text{EFF}}^2}, \quad \sigma_H = \frac{en_e}{B} \frac{\omega_{\text{ge}}^2\tau_{\text{EFF}}^2}{1 + \omega_{\text{ge}}^2\tau_{\text{EFF}}^2}, \quad (1)$$

$$D_{\perp} = \frac{k_B T_e}{eB} \frac{\omega_{\text{ge}}\tau_{\text{EFF}}}{1 + \omega_{\text{ge}}^2\tau_{\text{EFF}}^2}, \quad (2)$$

and the magnetic field diffusion coefficient [1],

$$D_B = \frac{\eta_{\text{EFF}}}{\mu_0} = \frac{B}{\omega_{\text{ge}}\tau_{\text{EFF}}en_e\mu_0}. \quad (3)$$

The Bohm-equivalent values are in all cases obtained at the value $\omega_{\text{ge}}\tau_{\text{EFF}} = 16$.

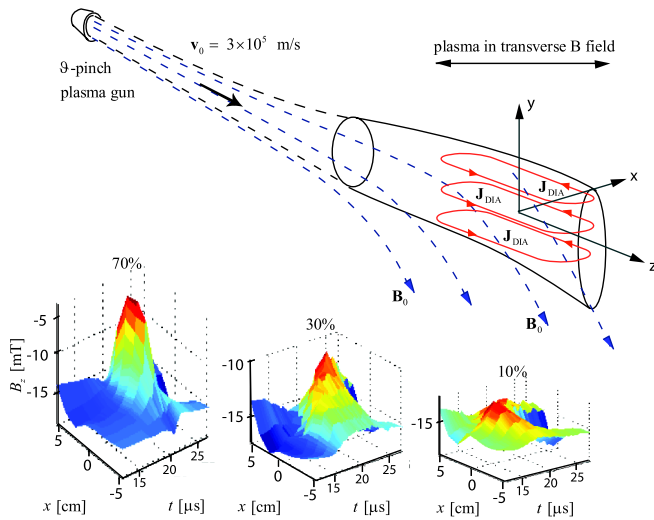


FIG. 3 (color online). Diamagnetic currents and fast magnetic diffusion in the plasma penetration experiment (adapted from [9]). The lower panels show the diamagnetic cavities that remain, $1 \mu\text{s}$ after entering the barrier, in three streams with different plasma densities.

Apparatus and experimental data.—The plasma penetration experiment is shown in Fig. 3, together with the magnetic cavities measured [9] in plasma streams of three different densities. From this experiment, two independent evaluations are made. The first is based on the process of magnetic diffusion into the plasma stream during the process of entering the region with transverse field. We have calculated the magnetic diffusion in a slab geometry, corresponding to the situation in a cut along the x axis of the plasma stream. The external magnetic field is ramped at a rate corresponding to the growth of the B_y component during the plasma penetration, and the diffusion equation $\partial B_y/\partial t = D_B(\partial^2 B_y/\partial x^2)$ is solved for the values of D_B that give closest to the three magnetic cavity profiles shown in Fig. 3. Equation (3) is then used to obtain the corresponding values of τ_{EFF} for Fig. 1. The error bars are drawn to be a factor of 2, based both on uncertainties in the plasma density and current density measurements, and on the fact that this represents an average over the width of the plasma stream. The second evaluation is the local resistivity calculation from the wave data as described in [9].

The sputtering magnetron geometry is shown in Fig. 4. We use data from three pulsed-power sputtering magnetron experiments [10,11,13], in which momentary power up to 300 kW was applied in short ($\leq 100 \mu\text{s}$) pulses. In these data the key measurements are of the azimuthal J_ϕ and discharge J_D current densities across \mathbf{B} , obtained by magnetic probes around current maximum. It follows from Eq. (1) that, when the currents J_ϕ and J_D are driven by electric fields, the current ratio directly gives $J_\phi/J_D = \sigma_H/\sigma_P = \omega_{\text{ge}}\tau_{\text{EFF}}$. In [11] it was shown that the relation $J_\phi/J_D = \omega_{\text{ge}}\tau_{\text{EFF}}$ holds also when J_ϕ and J_D are diamagnetic and electron diffusion currents, respectively, which are both driven by pressure gradients; according to [8] this dominates in the hot and dense plasma close to the cathode target. Independent of this uncertainty regarding the driving mechanism, $\omega_{\text{ge}}\tau_{\text{EFF}}$ can thus be obtained from mea-

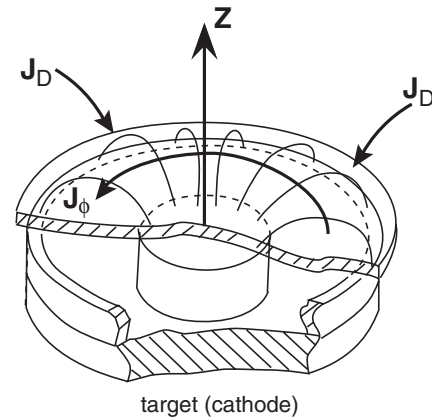


FIG. 4. A sputtering magnetron. Experiments from two different experiments in this geometry are analyzed, with pulsed power applied in the range 1.5–300 kW.

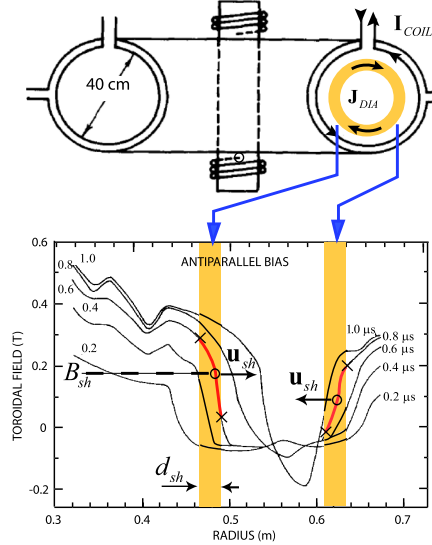


FIG. 5 (color online). The geometry of the toroidal theta pinch experiment, and magnetic profiles for the antiparallel ($\uparrow\downarrow$) bias case, adapted from [12]. The yellow shading marks the current sheaths that are used to evaluate τ_{EFF} for Fig. 1.

sured J_φ/J_D . Data at various distances from the target [13], and at discharge powers 1.5, 70, and 300 kW [10,11,13], all agree on values $J_\varphi/J_D \approx 2$, giving $\omega_{ge}\tau_{\text{EFF}} \approx 2$, and from that the values of τ_{EFF} plotted in Fig. 1. The error bars here represent estimates of the local variations around these volume averages.

The theta pinch from which we have taken data [12] is shown in Fig. 5, together with an example of magnetic profiles measured with arrays of small magnetic probes. The equation of magnetic diffusion, in the plasma rest frame, is [1] $\partial\mathbf{B}/\partial t = D_B\nabla^2\mathbf{B}$. Approximating the radial geometry of Fig. 5 as one-dimensional it gives

$$D_B = \frac{\partial B_\varphi}{\partial t} \frac{1}{\partial^2 B_\varphi / \partial r^2}. \quad (4)$$

As indicated in Fig. 5, the sheath's width d was approximated as the distance from 20% to 80% of full magnetic field change, and the speed u_{sh} as the speed of the sheath center in the laboratory rest frame. Approximating the time derivatives as $\partial B_\varphi / \partial t \approx u_{\text{sh}}(\partial B_\varphi / \partial r) \approx u_{\text{sh}}(B_{80\%} -$

$B_{20\%})/d$, and $\partial^2 B_\varphi / \partial r^2 \approx (B_{80\%} - B_{20\%})/d^2$, Eq. (4) reduces to $D_B \approx du_{\text{sh}}$ that, together with Eq. (3), gives $\tau_{\text{EFF}} \approx m_e/(e^2\mu_0 du_{\text{sh}} n_e)$. We have evaluated τ_{EFF} for the $\uparrow\downarrow$ and $\uparrow\uparrow$ bias cases, for the inner and outer sheaths, and at the times when the sheath middles ρ_1 are close to the half maximum of the density profile. This choice of time is a compromise where we avoid both the large uncertainties in n_e at larger radii and the final density compression by up to an order of magnitude close to the center.

This work was supported by the U.S. Department of Energy and the Swedish Research Council. Stimulating discussions with Mark Koepke, Ingvar Axnäs, and Tomas Hurtig are gratefully acknowledged.

- [1] F. F. Chen, *Introduction to Plasma Physics and Controlled Fusion*, Plasma Physics Vol. I (Plenum, New York, 1984), 2nd ed.
- [2] M. Bagatin *et al.*, J. Nucl. Mater. **266–269**, 771 (1999).
- [3] J. E. Maggs, T. A. Carter, and R. J. Taylor, Phys. Plasmas **14**, 052507 (2007).
- [4] C. C. Chaston, J. R. Johnson, M. Wilber, M. Acuna, M. L. Goldstein, and H. Reme, Phys. Rev. Lett. **102**, 015001 (2009).
- [5] M. Lyutikov and D. Uzdensky, Astrophys. J. **589**, 893 (2003).
- [6] Y. Uchiyama, F. A. Aharonian, T. Tanaka, T. Takahashi, and Y. Maeda, Nature (London) **449**, 576 (2007).
- [7] E. Parizot, A. Marcowith, J. Ballet, and Y. A. Gallant, Astron. Astrophys. **453**, 387 (2006).
- [8] N. Brenning, I. Axnäs, M. A. Raadu, D. Lundin, and U. Helmersson, Plasma Sources Sci. Technol. **17**, 045009 (2008).
- [9] N. Brenning, T. Hurtig, and M. A. Raadu, Phys. Plasmas **12**, 012309, (2005).
- [10] A. Vetushka and J. W. Bradley, J. Phys. D **40**, 2037 (2007).
- [11] D. Lundin, U. Helmersson, S. Kirkpatrick, S. Rohde, and N. Brenning, Plasma Sources Sci. Technol. **17**, 025007 (2008).
- [12] R. L. Merlino, G. C. Goldenbaum, C. Chin-Fatt, Y. P. Chong, A. W. DeSilva, H. R. Griem, R. A. Hess, and D. P. Murphy, Phys. Fluids **24**, 2358 (1981).
- [13] J. Bohlmark, U. Helmersson, M. VanZeeland, I. Axnäs, J. Alami, and N. Brenning, Plasma Sources Sci. Technol. **13**, 654 (2004).